Modern Physics Letters B
Vol. 36, No. 15 (2022) 2150610 (13 pages)

DOI: 10.1142/S0217984921506107

Calculating bandgaps of nonlinear mechanical metamaterials

Guoli Wang
Institute of Systems Engineering,
China Academy of Engineering Physics, Mianyang 621999, China

Shanwen Sun
Weichai Power Co., Ltd., Weifang 261061, Shandong, China

Ning An
School of Aeronautics and Astronautics, Sichuan University,
Chengdu 610065, China

Meie Li*
State Key Laboratory for Mechanical Behavior of Materials,
School of Materials Science and Engineering,
Xi'an Jiaotong University, Xi'an 710049, China
limeie@mail.xjtu.edu.cn

Jinxiong Zhou
State Key Laboratory for Strength and Vibration of Mechanical Structures,
Shaanxi Engineering Laboratory for Vibration Control of Aerospace Structures,
School of Aerospace Xi'an Jiaotong University, Xi'an 710049, China

Received 23 September 2021
Revised 14 November 2021
Accepted 8 December 2021
Published 14 June 2022

Bandgaps are intrinsic physical properties of periodic structures, for example, mechanical metamaterials or phononic crystals, which indicate attenuation of wave propagation within a specific frequency range. Bandgap calculation of mechanical metamaterials is realized via discretizing a representative voluame element (RVE) and imposing complex-valued Bloch wave boundary conditions. It is highly desirable to implement Bloch wave analysis in real-valued commercial finite element software. We present and detail an ABAQUS and Python implementation of Bloch wave analysis. Two-dimensional (2D) soft as well three-dimensional (3D) hard mechanical metamaterials are chosen as numerical examples. Material and geometric nonlinearities are tackled properly and the effects of pre-strains are explored. Our numerical results are validated either by similar results reported in the literature or by our experimental

*Corresponding author.

measurement. The presented numerical strategy would aid the design, analysis and utilization of mechanical metamaterials for dynamic applications. The codes and data of the paper could be downloaded from `https://github.com/XJTU-Zhou-group/Calculating-band-gaps-of-nonlinear-mechanical-metamaterials`.

Keywords: Bloch wave analysis; bandgap; mechanical metamaterial; finite element.

1. Introduction

Metamaterials are man-made materials that obtain their unusual properties by structure rather than chemistry. Metamaterials have evolved from electromagnetic, acoustic, optical and thermal[1–5] to more recent and vibrant mechanical ones.[6–13] Mechanical metamaterials are rationally designed artificial materials whose unconventional effective properties or macroscopic behaviors are achieved through exploiting motion, deformation, stress and mechanical energy of its building blocks.[13] For example, a piece of polymeric block with array of holes exhibits negative Poisson's ratio when it is compressed.[14–16] Other zero or negative material parameters such as density, elastic moduli and compressibility can also be achieved.

With the help of advanced three-dimensional (3D) printing technology, research on mechanical metamaterials has succeeded in efforts to create metamaterials with complicated structures and a variety of soft and hard materials including polymer, plastics, metals and ceramics. Recent designs of novel mechanical metamaterials incorporating origami creases, kirigami cuts, topological protection, snapping-through elements and negative-stiffness inclusions exhibit very sophisticated mechanical behavior through shape morphing, topological protection, instabilities and nonlinear responses, and call for high-fidelity nonlinear finite element analysis involving contact, instability, geometric and material nonlinearity.[9–13]

Dynamics is at the heart of behavior of mechanical metamaterials; the long-standing interests originate from earlier work on dynamics of wave-based and acoustic metamaterials to more recent work on non-reciprocal wave propagation and low frequency vibration control.[7,10,17,18] Dynamics of periodic mechanical metamaterials or closely related phononic crystals is compactly described by their bandgaps or dispersion relations, and thus calculating bandgap is a task of top priority for dynamics of mechanical metamaterials.[19–23]

The theory for calculating bandgaps of periodic structures lays its basis on Bloch theorem which states that for any periodic structure the change in complex wave amplitude across a unit cell does not depend upon the location of the unit cell within the structure.[19,20] Therefore, one can analyze wave propagation through the entire structure by only considering wave motion within a single unit cell, resulting in enormous savings in computation time and computer storage. The process of enforcing Bloch boundary conditions within a single unit cell and performing frequency analysis is called Bloch wave analysis. Besides bandgap calculation, Bloch wave analysis is also a powerful technique to determine the critical load for onset of buckling and wrinkling of elastic media.

To invoke Bloch theorem, one admits complex valued plane wave solution for displacement and enforcing periodic boundary conditions on the outer surfaces of the unit cell. This process can be implemented by home-made finite element codes. However, it would be desirable to be able to use commercial finite element software due to its powerfulness of pre- and post-processing, robustness of algorithm and automatic computation of mass and stiffness matrices.[20] Usage of commercial software also facilitates interaction between academia and industry community. Unfortunately, the most popular commercial finite element software, such as ABAQUS, ANSYS and NASTRAN, are programmed for real valued field equations. There is an exception, COMSOL, for multiphysics simulation. COMSOL is amenable to complex valued equations and therefore exclusively used for bandgap of phononic crystals and mechanical mematerials with small deformations. Nevertheless, its limitation in nonlinear analysis is well-known, and as such, it is not well-suited for nonlinear analysis and bandgap calculation of complex periodic structures.

ABAQUS is very popular and extensively used in solid mechanics community. Its strong capability in nonlinear finite element analysis is widely acknowledged and most trusted. Here, we describe and detail an ABAQUS and Python implementation of Bloch wave analysis for bandgap computation of two-dimensional (2D) soft polymeric metamaterials with periodic holes as well as 3D hard metamaterials. The real valued Bloch boundary conditions and the associated eigenvalue problem are treated via a user programmed multiple point constraint, UMPC, over two identical meshes — one for the real part and one for the imaginary part. All the Python files for ABAQUS as well as the UMPC codes are provided in the supporting information of the paper. Our efforts enrich the analysis tools for dynamics of mechanical metamaterials, and can also be used straightforwardly for bandgap calculation of other periodic structures.

2. Bloch Wave Analysis for a Periodically Structured Solid with Finite Deformation

Let us consider a material particle $\mathbf{X}$ that undergoes a finite deformation and deforms to $\mathbf{x}$ such that a deformation gradient is defined as

$$\mathbf{F} = \frac{\partial \mathbf{x}}{\partial \mathbf{X}}. \tag{1}$$

The equation of motion of the solid without body force is expressed in the undeformed configuration as

$$\nabla_0 \cdot \mathbf{S} = \rho_0 \frac{D^2\mathbf{X}}{Dt^2}, \tag{2}$$

where ∇_0 and ρ_0 are the gradient operator and the density defined in reference configuration, $\mathbf{S}$ denotes the first Piola–Kirchoff stress tensor and $\frac{D}{Dt}$ is the material time derivative. Letting the right-hand side acceleration term equal to zero, Eq. (2) recovers the static equilibrium equation.

Consider a perturbation superposed on an equlibrium state with finite deformation, the increment also satisfies the equation

$$\nabla_0 \cdot \dot{\mathbf{S}} = \rho_0 \frac{D^2 \dot{\mathbf{x}}}{Dt^2}, \tag{3}$$

where dots denote increments; increment of stress tensor $\dot{\mathbf{S}}$ is related to increment of deformation gradient $\dot{\mathbf{F}}$ through a linearized constitutive law, i.e. $\dot{\mathbf{S}} = \mathbf{L}{:}\dot{\mathbf{F}}$, with $\mathbf{L}$ a fourth-order tensor representing the linearized stiffness. If a plane wave solution is admitted, an incremental wave with frequency is characterized by

$$\dot{\mathbf{x}}(\mathbf{X}, t) = \dot{\mathbf{Q}}(\mathbf{X}) \exp(-i\omega t), \tag{4}$$

where $\dot{\mathbf{Q}}$ is the incremental displacement and the stress is also complex valued

$$\dot{\mathbf{S}} = \dot{\Sigma} \exp(-i\omega t). \tag{5}$$

Plugging equations (4) and (5) into Eq. (3) yields

$$\nabla_0 \cdot \dot{\Sigma} + \rho_0 \omega^2 \dot{\mathbf{Q}} = 0. \tag{6}$$

To calculate bandgaps of a periodic structure using commercial finite element software like ABAQUS, the majority of which only permit real-valued field variables, all fields are split into real and imaginary parts, and thus in this way, the incremental equation (6) is split into two sets of equations for the real and imaginary parts,[20–23]

$$\nabla_0 \cdot \dot{\Sigma}^{\mathrm{RE}} + \rho_0 \omega^2 \dot{\mathbf{Q}}^{\mathrm{RE}} = 0, \tag{7}$$

$$\nabla_0 \cdot \dot{\Sigma}^{\mathrm{IM}} + \rho_0 \omega^2 \dot{\mathbf{Q}}^{\mathrm{IM}} = 0. \tag{8}$$

A periodically structured solid can be constructed by selecting a representative volume element (RVE) and tessellating the RVE along the basis vectors of direct lattice $\mathbf{a}_i$. According to Bloch's theorem, any space function satisfies the periodic boundary conditions

$$\Psi(\mathbf{X} + \mathbf{R}) = \Psi(\mathbf{X}) \exp[i\mathbf{k} \times \mathbf{R}], \tag{9}$$

where vector $\mathbf{R}$ is obtained by n_i translations along the $\mathbf{a}_i$ directions with n_i being integers

$$\mathbf{R} = n_1 \mathbf{a}_1 + n_2 \mathbf{a}_2 + n_3 \mathbf{a}_3 \tag{10}$$

and $\mathbf{k}$ is the wave vector. A counterpart of $\mathbf{a}_i$, the so-called basic vectors of reciprocal lattice $\mathbf{b}_i$ is also introduced in such a way that $\mathbf{a}_i \cdot \mathbf{b}_j = 2\pi\delta_{ij}$ with δ_{ij} being Kronecker delta function. Wave vector $\mathbf{k}$ can be expressed in terms of either $\mathbf{a}_i$ or $\mathbf{b}_i$.

Bandgaps are thus calculated by constructing two identical meshes for the RVE-one for the real part and one for the imaginary part-and coupling them by imposing the following Bloch-type displacement boundary conditions:

$$\dot{\mathbf{Q}}^{\mathrm{RE}}(\mathbf{X} + \mathbf{R}) = \dot{\mathbf{Q}}^{\mathrm{RE}}(\mathbf{X}) \cos[\mathbf{k} \cdot \mathbf{R}] - \dot{\mathbf{Q}}^{\mathrm{IM}}(\mathbf{X}) \sin[\mathbf{k} \cdot \mathbf{R}], \tag{11}$$

$$\dot{\mathbf{Q}}^{\mathrm{IM}}(\mathbf{X} + \mathbf{R}) = \dot{\mathbf{Q}}^{\mathrm{RE}}(\mathbf{X}) \sin[\mathbf{k} \cdot \mathbf{R}] + \dot{\mathbf{Q}}^{\mathrm{IM}}(\mathbf{X}) \cos[\mathbf{k} \cdot \mathbf{R}]. \tag{12}$$

Discretizing Eqs. (7) and (8) by the finite element method and applying boundary conditions (11) and (12), the eigenfrequencies ω are obtained for any given wave vector $\mathbf{k}$. Imposing of boundary conditions (11) and (12) are realized by programming a user programmed multiple point constraint, UMPC and the Bloch wave analysis is performed by a Python script in ABAQUS (Supporting information). This procedure is applicable for materials undergoing finite deformation, and also applicable for bandgap calculation of any periodic structures.

3. Bandgap Calculation of a 2D Soft Mechanical Metamaterial

We choose here a 2D soft mechanical metamaterial made of rubber undergoing finite deformation. The analysis of this type of mechanical metamaterials involves material nonlinearity as well as geometric nonlinearity, and serves as an excellent example to demonstrate the effectiveness of the proposed numerical strategy. Here, we consider a neo-Hookean hyperelastic material with shear modulus $G = 1.1$ Mpa, bulk modulus $K = 2.0$ GPa, Poisson's ratio $\mu = 0.4997$ and density $\rho = 1050\ \mathrm{kg/m^3}$. Figure 1(a) shows an infinite periodically structured elastomer sheet with an array of perforated holes. Figure 1(b) gives the $L \times L$ ($L = 20$ mm) RVE with two different hole radii, $R1 = 4.57$ mm and $R2 = 4.16$ mm, marked in the figure. The RVE was discretized by 9520 six-node plane strain, hybrid, quadratic triangular elements (Abaqus element type CPE6H). Figures 1(a) and 1(c) also give the basic vectors defined in direct lattice (a) and reciprocal lattice (c). The shaded area in Fig. 1(c) is the first Brillouin zone in reduced wave vector space.

The primary interest here is to probe the effect of applied pre-strain on the bandgap structure of the soft mechanical metamaterial. Figure 2 plots various

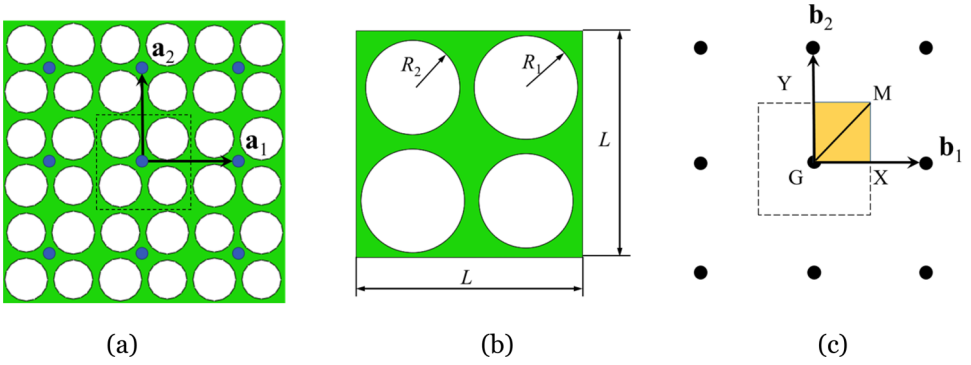

Fig. 1. (Color online) Bloch wave analysis model of a 2D soft mechanical metamaterial. (a) An infinite periodically structured elastomer sheet with an array of holes with two different sizes. Basic vectors of direct lattice $\mathbf{a}_i$ are shown herein and the domain enclosed by the black dashed line is the RVE. (b) A $L \times L$ square RVE perforated with four holes with two different radii denoted by $R1$ and $R2$, respectively. (c) The basic vectors of reciprocal lattice and the corresponding irreducible first Brillouin zone (shaded orange region GXM).

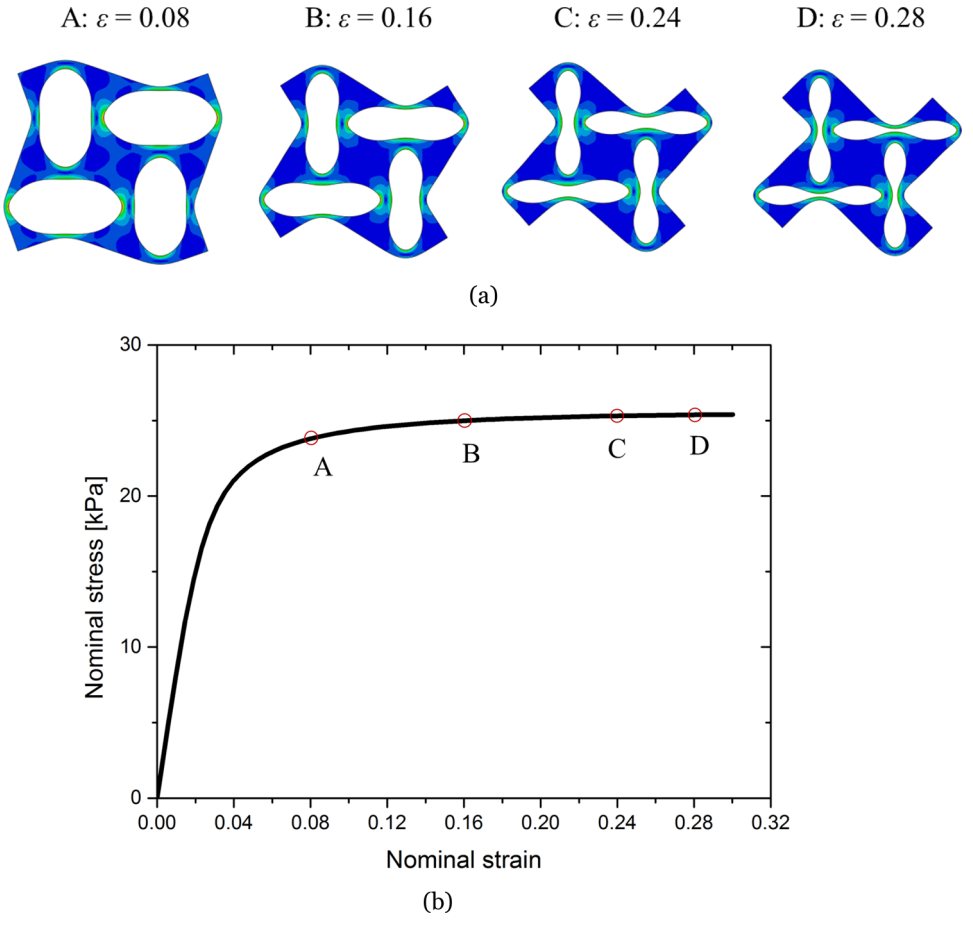

Fig. 2. (Color online) Deformation process and stress–strain curve of the RVE for various applied strains ε. (a) Various deformation states of the RVE for applied strains $\varepsilon = 0.08$, 0.16, 0.24 and 0.28 marked by A, B, C and D, respectively. (b) The nominal strain versus nominal stress curve.

deformation states and the corresponding stress–strain curve of the RVE, with various applied strains 0.08, 0.16, 0.24 and 0.28 and corresponding states marked by A, B, C and D, respectively. Figures 3(a) and 3(b) plots and compares two bandgaps of the RVE without (a) and with applied strain 0.28 (b). A noticeable difference lies in the fact there is only one bandgap for metamaterial without pre-strain, frequencies from 2000 Hz to 2600 Hz, whereas there exist four bandgaps for the material with applied 0.28 compressive strain in vertical direction. Besides the primary bandgap from 2000 Hz to 2600 Hz, there are additional three narrow bandgaps around 1400, 3300 and 6000 Hz. To quantitatively investigate the influence of applied strain on the bandgaps, Fig. 3(c) plots the variation of mid-gap frequency and the bandgap width, which are defined as $(f_L + f_U)/2$ and $\frac{2(f_U - f_L)}{(f_L + f_U)}$, respectively, f_L and f_U being

lower and upper frequencies of a bandgap. Figure 3(d) plots the distribution of bandgap frequency over various applied compressive strains. Figure 3(d) coincides with the results presented in Figs. 3(a) and 3(b), indicating that imposing compressive strain entails increase of distribution of bandgaps. A physical understanding of this phenomenon is that applying compressive stress in an elastic body softens the elastic and reduces its stiffness, eventually modifies its natural frequency distribution. Note that similar results in Fig. 3 are given by Bertoldi *et al.*[22,23] for

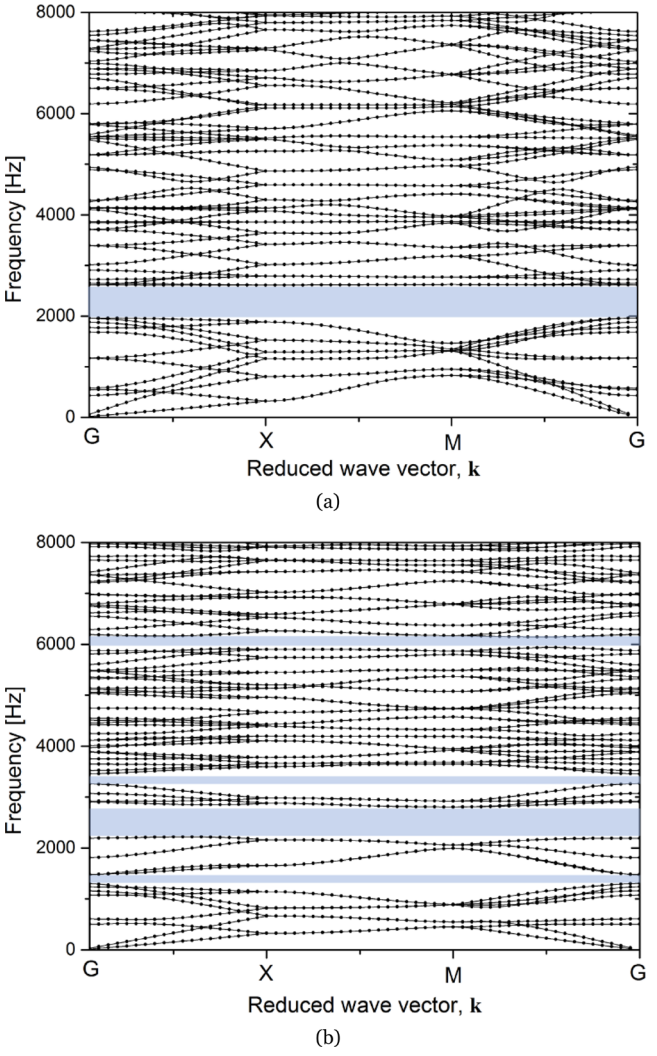

Fig. 3. (Color online) Bandgap structure of a 2D soft mechanical metamaterial without (a) and with applied pre-strain 0.28 (b). (c) Variation of mid-gap frequency and bandgap width with applied nominal strain. (d) Distribution of bandgap frequency over various applied compressive strains.

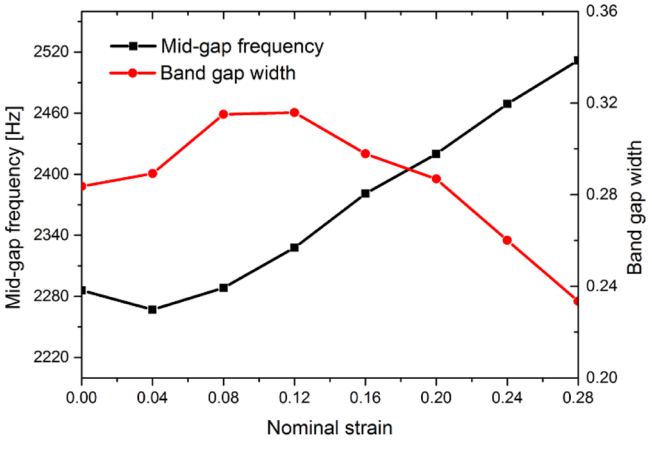

(c)

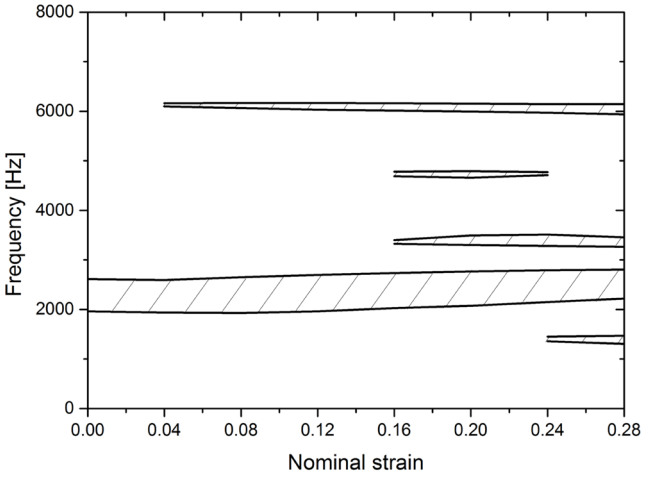

(d)

Fig. 3. (*Continued*)

elastomeric phononic crystals undergoing large deformation, which partially validates our implementation.

4. Bandgap Calculation of a 3D Hard Mechanical Metamaterial

Figure 4 shows the design and CAD drawing of a 3D mechanical metamaterial and its RVE for bandgap calculation. Also shown herein is the definition of the wave vector coordinates and the irreducible first Brillouin zone (the tetrahedron ΓRXM). The mechanical metamaterial is similar to the phononic crystal developed by D'Alessandro *et al.*[18] and consists of beams with spherical lumped masses. The RVE is a $L \times L \times L$ cube with square cross-sections $W/2 \times W/2$ (the cross-section of the metamaterial is $W \times W$ with $W = 3.2$ mm). The radius of the lumped sphere is

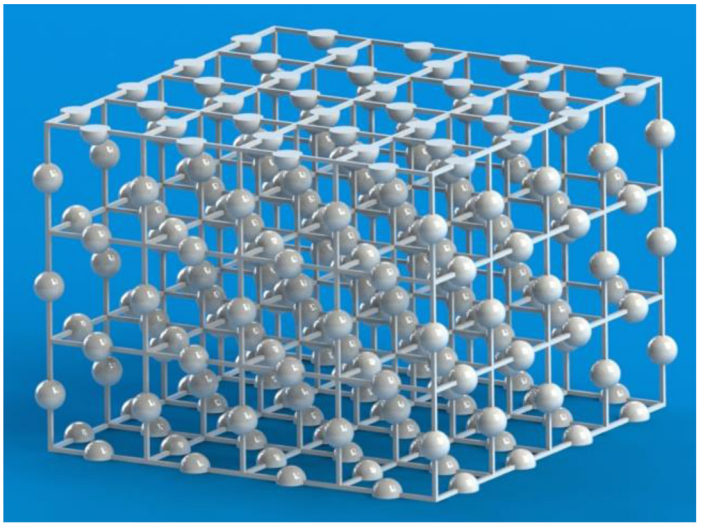

(a)

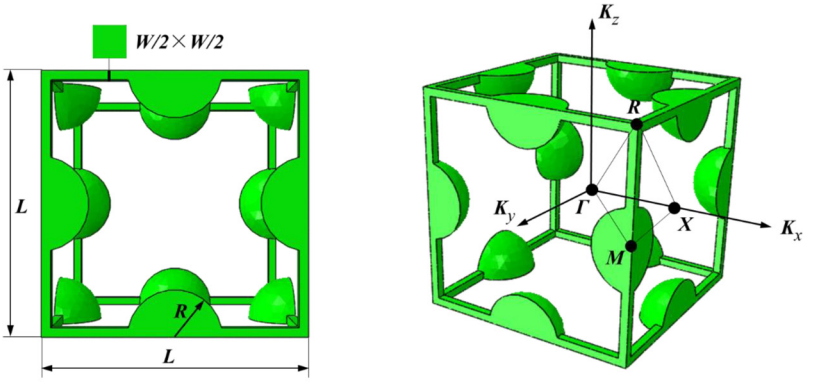

(b)

Fig. 4. (Color online) The CAD drawing of a 3D mechanical metamaterial and its RVE for bandgap calculation. (a) CAD drawing of a 3D mechanical metamaterial. (b) RVE of the 3D mechanical metamaterial (left) and the wave vector and the irreducible first Brillouin zone (the tetrahedron ΓRXM).

$R = 8$ mm. The mechanical metamaterial is made of curable resin (sterelithography material, DSM product, Somos Imagine 8000) with Young's modulus $E = 2.48$ GPa, Poisson's ratio $\mu = 0.41$ and density $\rho = 1100$ kg/m^3.

The RVE was discretized by 89,834 3D four-node linear tetrahedral elements (Abaqus element type C3D4), and the accuracy of the mesh was ascertained through a mesh refinement study. Due to structural symmetry, eigenvalue problem was solved along the boundary of irreducible first Brillouin zone, ΓRXM, which was

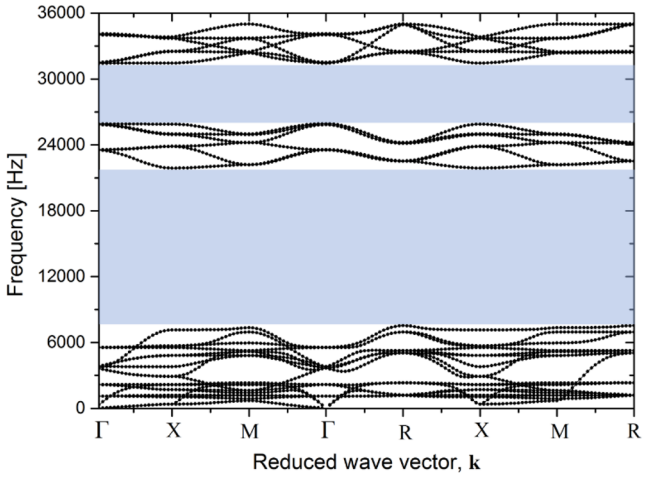

(a)

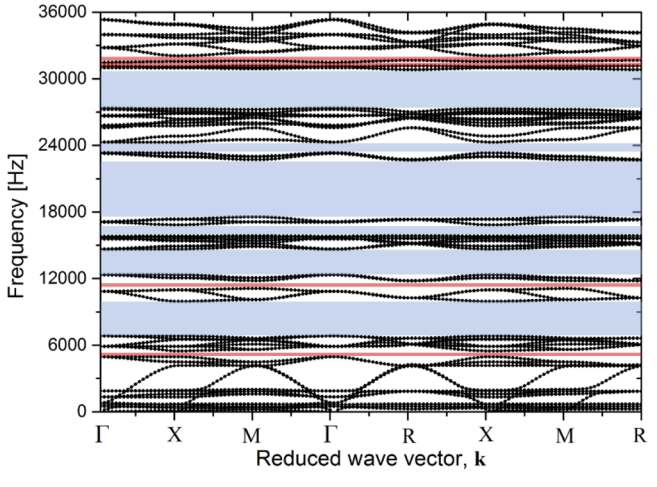

(b)

Fig. 5. (Color online) Bandgaps of a 3D hard mechanical metamaterials ((a) $L = 35.2$ mm; (b) $L = 73.2$ mm).

discretized by 20 points. Bandgaps with various lengths of RVE were calculated and Fig. 5 shows two of the bandgap structures, corresponding to $L = 35.2$ mm and 73.2 mm, respectively. In Fig. 5(a) with $L = 35.2$ mm, there exist two bandgaps, one in the range of 7532 Hz–21,884 Hz and one in the range of 25,930–31,420 Hz. For the case with larger length of RVE, $L = 73.2$ mm, there exist six main bandgaps marked by shaded gray color, in addition to several narrow bandgaps in red color. This example demonstrates that achieving desirable bandgap distribution is possible by designing configurations and tailoring parameters of RVE.

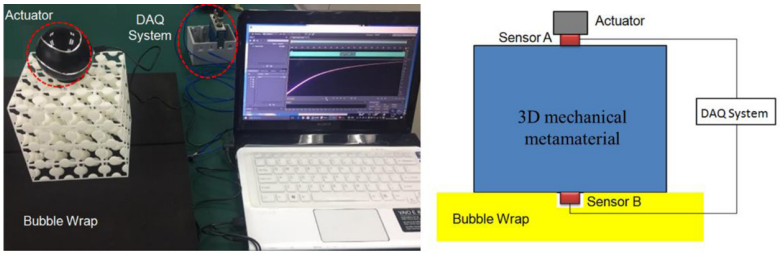

(a)

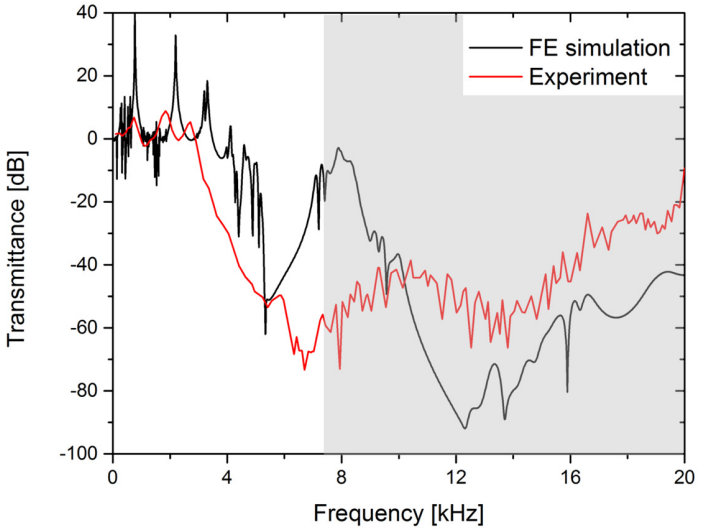

(b)

Fig. 6. (Color online) Experimental measurement of the vibration transmittance of a 3D mechanical metamaterial fabricated by 3D printing. (a) Experimental setup. (b) Transmittance.

To further verify the correctness of our numerical method, we adopted the identical experimental setup used by D'Alessandro *et al.*[18] and performed experimental measurement of the 3D printed mechanical metamaterial with $L = 35.2$ mm. Figure 6(a) shows the picture of the experimental setup, and the vibration transmission is measured. The fabricated mechanical metamaterial was placed on a soft bubble wrap with a sensor A and a sensor B attached on the top and bottom surfaces of the metamaterials, respectively. A DAQ system was used to acquire the acceleration data. The metamaterial was excited by a vibration shaker Vibe-Tribe Troll, and the acceleration sensors were PCB Piezotronics 353B15. Figure 6(b) plots the vibration transmittance defined by $T = 20 \log \| \frac{A_{\text{out}}(\omega)}{A_{\text{in}}(\omega)} \|$, where A_{out} is the output sample given by sensor B while A_{in} is the input sample given by sensor A. It is shown in Fig. 6(b) that the experimentally measured vibration transmittance of the finite-size 3D metamaterial (red line) matches well with the data predicted

by finite-size vibration transmittance simulation (black line), both being in a good agreement with the bandgap predicted by the RVE bandgap calculation (gray area).

5. Concluding Remarks

Mechanical metamaterials are artificial materials whose peculiar properties depend on their size and arrangement of unit cells rather than the chemistry of constituent materials. Efforts are devoted in developing mechanical metamaterials for diverse applications, among them the application of mechanical metamaterials for dynamics control and vibration isolation is a flourishing interest. Bandgap structure of a mechanical metamaterial with periodic unit cell reflects the range of frequencies in which harmonic wave propagation is blocked, therefore, calculation of bandgap structure is at the core of dynamics of mechanical metamaterials.

Mechanical metamaterials are typically fabricated by the cutting-edge technology of 3D printing and, to date, majority of them are made of polymer-like materials with nonlinear properties. Deformation of mechanical metamaterials usually involves finite deformation and geometric nonlinearity. To accurately capture the bandgaps of these mechanical metamaterials, nonlinear finite element software are desperately needed, most of them only deal with real-valued field variables.

To this end, we present in this paper an implementation strategy of bandgap calculation in ABAQUS in together with Python script and user subroutine multiple point constraint. A 2D elastomeric sheet with an array of holes with two different sizes of radii was chosen as the first example. Hyperelastic material nonlinearity and large deformation are incorporated in this example. Focus is placed on the effect of applied compressive strain on the distribution and evolution of bandgaps of this 2D mechanical metamaterial. The overall trend of the presented 2D examples follows the similar behavior reported in the literature for soft phononic crystals with large deformation. With the success of the 2D example, we extend the bandgap calculation of 3D mechanical metamaterials. Bandgap of a 3D beam-in-mass lattice structure is obtained. The numerical results of 3D hard metamaterials are compared with the experiments performed over 3D printed samples and good agreement is achieved. Our efforts presented herein enrich the analysis of mechanical metamaterials and phononic crystals, and also pave the way for the design and fabrication of mechanical metamaterials.

Acknowledgments

This research is supported by Natural Science Foundation of China (Grant No. 11972277), and by a technological project of Institute of Systems Engineering, China Academy of Engineering Physics (2017KJZ06).

References

1. M. Kadic *et al.*, *Rep. Prog. Phys.* **76**(12) (2013) 126501.
2. J. Valentine *et al.*, *Nature* **455**(7211) (2008) 376.

3. J. Mei *et al.*, *Nat. Commun.* **3** (2012) 756.
4. S. A. Cummer, J. Christensen and A. Alù, *Nat. Rev. Mater.* **1**(3) (2016) 16001.
5. S. Narayana and Y. Sato, *Phys. Rev. Lett.* **108**(21) (2012) 214303.
6. X. Zheng *et al.*, *Science* **344**(6190) (2014) 1373.
7. P. Wang *et al.*, *Phys. Rev. Lett.* **113**(1) (2014) 014301.
8. B. Florijn, C. Coulais and M. van Hecke, *Phys. Rev. Lett.* **113**(17) (2014) 175503.
9. T. Frenzel, M. Kadic and M. Wegener, *Science* **358**(6366) (2017) 1072.
10. C. Coulais, D. Sounas and A. Alù, *Nature* **542**(7642) (2017) 461.
11. J. L. Silverberg *et al.*, *Science* **345**(6197) (2014) 647.
12. C. Coulais *et al.*, *Nature* **535**(7613) (2016) 529.
13. K. Bertoldi *et al.*, *Nat. Rev. Mater.* **2**(11) (2017) 17066.
14. K. Bertoldi *et al.*, *Adv. Mater.* **22**(3) (2010) 361.
15. K. Bertoldi *et al.*, *J. Mech. Phys. Solids* **56**(8) (2008) 2642.
16. G. Wang, M. Li and J. Zhou, *Soft Mater.* **14**(3) (2016) 180.
17. K. H. Matlack *et al.*, *Proc. Natl. Acad. Sci.* **113**(30) (2016) 8386.
18. L. D'Alessandro *et al.*, *Appl. Phys. Lett.* **109**(22) (2016) 221907.
19. A. S. Phani, J. Woodhouse and N. A. Fleck, *J. Acoust. Soc. Amer.* **119**(4) (2006) 1995.
20. M. Åberg and P. Gudmundson, *J. Acoust. Soc. Amer.* **102**(4) (1997) 2007.
21. K. Bertoldi and M. C. Boyce, *Phys. Rev. B* **77**(5) (2008) 052105.
22. K. Bertoldi and M. C. Boyce, *Phys. Rev. B* **78**(18) (2008) 184107.
23. L. Wang and K. Bertoldi, *Int. J. Solids Struct.* **49**(19–20) (2012) 2881.